Letter

Neutron versus proton scattering on exotic nuclei: The ^{9}He example

M. S. Khirk [1,*] L. V. Grigorenko [1,2,3] D. E. Lanskoy [4] and P. G. Sharov [1,5]

[1]*Flerov Laboratory of Nuclear Reactions JINR, 141980 Dubna, Russia*
[2]*National Research Nuclear University MEPhI, 115409 Moscow, Russia*
[3]*National Research Centre "Kurchatov Institute," 1 Kurchatov Square, 123182 Moscow, Russia*
[4]*Faculty of Physics, Lomonosov Moscow State University, Leninskie Gory, Moscow, 119991, Russia*
[5]*Institute of Physics in Opava, Silesian University in Opava, 74601 Opava, Czech Republic*

(Received 3 March 2025; accepted 22 April 2025; published 19 May 2025)

Neutron scattering on exotic nuclides is a class of processes that cannot be studied directly now and in any foreseeable future. Resonance proton scattering of exotic nuclide on a thick target in inverse kinematics can be used to infer the properties of the low-energy neutron scattering of this nuclide, assuming the isobaric symmetry. However, the results of such resonance proton scattering reactions have so far been analyzed in theoretical approaches (optical, R-matrix models), which are missing important aspects of isospin dynamics, isospin violation in continuum, and threshold dynamics. The isospin-conserving coupled-channel model (ICM) is proposed, providing a more reliable basis for understanding such experimental studies. Qualitatively different phase shifts for the ^{8}He $+p$ $T = 5/2$ and $T = 3/2$ resonances are predicted by ICM with a quite unusual profile for the $T = 5/2$ states. An alternative interpretation of the existing ^{8}He $+p$ data is proposed. The observable properties of the $T = 5/2$ resonances may be strongly affected by the isobaric-partner $T = 3/2$ states. The crucial importance of studies of the neutron-emission channel for disentangling this possible influence is demonstrated.

DOI: 10.1103/PhysRevC.111.L051601

Introduction. Resonance proton scattering (RPS) on a thick target in inverse kinematics is an elegant and powerful experimental method [1]. It was found especially efficient for studies with exotic radioactive beams of low quality and intensity, because very thick targets can be used: the low-energy elastic scattering excitation functions in a broad energy range and corresponding angular distributions are obtained simultaneously with a fixed-energy incoming beam. The application of the method is very natural for the proton continuum of *proton-rich* exotic nuclei, where the interpretation of elastic scattering results is straightforward and unique [1–5].

Another application of the method presumes getting information on the neutron scattering of some *neutron-rich* exotic nuclide $^{A}Z+n$ by studying the "isobaric partner reaction" of proton scattering $^{A}Z+p$. For each spin-parity J^{π}, the observed isobaric-analog state (IAS) in the $^{A}Z+p$ channel with $\{T = T_{\max}, T_3 = T_{\max} - 1\}$ is described by some theoretical model. By switching off the Coulomb interaction in the $^{A}Z+p$ channel, the properties of the $^{A}Z+n$ continuum with $\{T = T_{\max}, T_3 = T_{\max}\}$ are deduced [6–11].

The results of ^{8}He $+p$ studies targeting ^{9}He properties were analyzed in models (optical potential, R-matrix) [6,10] which have some room for the phenomenological treatment of channel coupling but are missing specific aspects of isospin dynamics connected with isospin conservation. The following issues are shown in this work to be important specifically for ^{8}He $+p$ studies and may be important for an application of the RPS method in general:

(i) The continuum states in the $^{A}Z+p$ channel with $\{T = T_{\max}, T_3 = T_{\max} - 1\}$ are typically "globally" (i.e., in the whole radial space) isospin-mixed. This is always true for ^{A}Z systems with nonzero total isospin. For such cluster-continuum configurations, the good quantum number of isospin is recovered "locally" (in some radially limited "nuclear interior"). To make this recovery possible, mixing the $^{A}Z+p$ channel with the $^{A}(Z+1, \mathrm{IAS})+n$ channel is needed. In our ^{9}He case, these are ^{8}He$(0^{+}2)+p$ and ^{8}Li$^{*}(0^{+}2)+n$ channels. The aspect of this mixing governed by the isospin conservation can be reliably modelled.

(ii) The pure isospin concept is perfect for zero-width discrete states and quite precise for small-width continuum states. The states in the dripline neutron-rich systems—e.g., ^{9}He $=$ ^{8}He $+n$—are expected to be quite broad. This means that the corresponding states in the ^{8}He $+p$ continuum should be even broader. There is a certain isospin-symmetry-violation aspect of nuclear dynamics, which is connected only with the large width of the considered states: broad states with definite isospin are more strongly coupled to both ^{8}He$(0^{+}2)+p$ and ^{8}Li$^{*}(0^{+}2)+n$ continuums. Neither of these continuums has definite isospin. Therefore, the isospin mixing stemming from the

*Contact author: mskhirk@jinr.ru

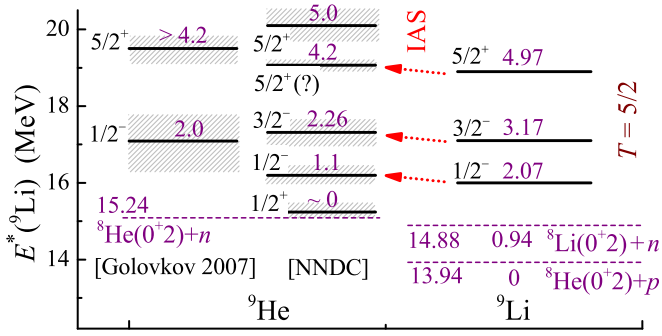

FIG. 1. Relevant levels in ^{9}He and ^{9}Li systems. The data of [12] is shown separately, since it is quite different from the NNDC vision of the low-lying negative-parity states.

continuum couplings becomes more important as the considered states grow broader.

(iii) Mixing the ${}^AZ+p$ and ${}^A(Z+1,\mathrm{IAS})+n$ channels presumes that, together with the $T = T_{\max}$ IAS state, an "isobaric partner" state with $T = T_{\max} - 1$ may exist nearby in energy. In the spectra of ^{4}He and ^{8}Be, such isospin doublets are known and well-studied, e.g., in [13,14] and references therein. In the case of insufficient energy separation, the "isobaric partner" state should significantly affect the observable properties of the ${}^AZ+p$ IAS state. We show in this work that, for states broader than $\Gamma \gtrsim 0.3$ MeV, any realistic energy gap between them is insufficient enough to make their interference negligible. This makes the interpretation of the proton-scattering data on broader states in terms of isolated resonances unreliable.

(iv) In the light nuclei, the thresholds of the ${}^AZ+p$ and ${}^A(Z+1,\mathrm{IAS})+n$ channels are typically located just within ~ 1 MeV of energy. For broad states, complicated threshold dynamics may take place around these thresholds. For example, dynamical studies of these phenomena in the coupled-channel model are absolutely essential for understanding $l = 0$ states: they are represented by *resonances* in the ${}^AZ+p$ continuum, but by *virtual states* ${}^AZ+n$ and ${}^A(Z+1,\mathrm{IAS})+n$ channels, that make the situation extremely complicated for interpretation.

The above aspects of isospin dynamics can be accounted consistently in a relatively simple coupled-channel model. Such an isospin-conserving model was developed and successfully applied during studies of the isospin mixing in ^{4}He and ^{8}Be systems in Refs. [13,14]. We demonstrate below that, based on such a model, the experimental data may be interpreted very differently, and, moreover, a reliable interpretation is possible only if the ${}^AZ+p$ scattering data is augmented with the neutron-emission ${}^A(Z+1,\mathrm{IAS})+n$ channel data.

Understanding the ^{9}He *spectrum* is quite controversial, see a good summary of the data in [15], additional recent data in [16], and Fig. 1. This is important motivation for using the ^{9}He system as an example.

There is some common agreement about positioning the $5/2^+$ state but with quite a large energy uncertainty $E_r \sim 3.4 - 5.2$ MeV. There is also some common agreement about positioning the $1/2^-$ state $E_r \sim 1.1 - 1.3$ MeV. However, the only work that provides a spin-parity identification positions $1/2^-$ quite differently with $E_r = 2 \pm 0.2$ MeV [12]. The NNDC prescription (see also [17]) for the $T = 5/2$ states located high in the ^{9}Li continuum comes only from the ^{8}He $+p$ data of Ref. [6]. Also, the possibility of the low-lying $3/2^-$ state in ^{9}He was inferred based on these data.

The possibility of the low-lying $1/2^+$ has been considered many times in the literature since some evidence for a large negative scattering length $a_s < -10$ fm was found in Ref. [18]. Nevertheless, the situation remains uncertain. On the one hand, a low-lying structure, corresponding to $a_s \approx -12 \pm 3$ fm, was reported in [15]. On the other hand, no "strong" virtual state in ^{9}He was found in Refs. [19,20] providing the scattering lengths $a_s \approx -3$ fm and $a_s \gtrsim -3$ fm, correspondingly. Also, in Ref. [21], the large negative scattering length, e.g., as large as $a_s \approx -20$ fm, is not completely excluded in principle but is highly unfavorable. In the analysis of [16], the ^{8}He $+n$ final state interaction allows both modest $a_s \sim -2$ fm and relatively strong $a_s \sim -10$ fm, depending on assumptions. Theoretical analysis of [22] based simultaneously on the ^{9}He and ^{10}He data provides the limitation $a_s \gtrsim 1$ fm.

A vision of the ^{9}He spectrum that differs greatly from anything listed above is proposed based on the ^{8}He $+p$ data in Ref. [10]: the $1/2^+$ resonance at $E_r \sim 3$ MeV with, simultaneously, no room for the low-lying p-wave resonance with $E_r \lesssim 2.0 - 2.5$ MeV.

In light of the long-term confusion concerning the ^{9}He spectrum, the additional ^{8}He $+p$ data may provide crucial missing information. However, this information can be extracted from the data only if the isospin mixing issues are, theoretically, reliably resolved.

Isospin-conserving model for the ^{8}He *-p reaction.* Let us rewrite model [13] for the ^{8}He $+p$ resonance scattering reaction. For the $^8\mathrm{He}(0^+2)+p$ and $^8\mathrm{Li}^*(0^+2)+n$ channels, the assumption of isospin symmetry leads to interaction between clusters which can be represented as a sum of terms with definite isospin:

$$\hat{V} = V_{3/2}(r)\,\hat{P}_{3/2} + V_{5/2}(r)\,\hat{P}_{5/2},$$

where $\hat{P}_T$ are projection operators on the states with definite total isospin T. The cluster WFs with definite asymptotic conditions are connected to WFs with definite isospin $|T, T_3\rangle$ as

$$\begin{aligned}\Psi_{^8\mathrm{He}\text{-}p} &= \frac{1}{\sqrt{5}}|5/2, 3/2\rangle + \frac{2}{\sqrt{5}}|3/2, 3/2\rangle\\ \Psi_{^8\mathrm{Li}^*\text{-}n} &= \frac{2}{\sqrt{5}}|5/2, 3/2\rangle - \tfrac{1}{\sqrt{5}}|3/2, 3/2\rangle.\end{aligned} \tag{1}$$

From this decomposition, it is clear that the coupling of the scattering ^{8}He $+p$ channel to the $T = 5/2$ is relatively weak, which appears to be very important (see Fig. 4 and the discussion around it).

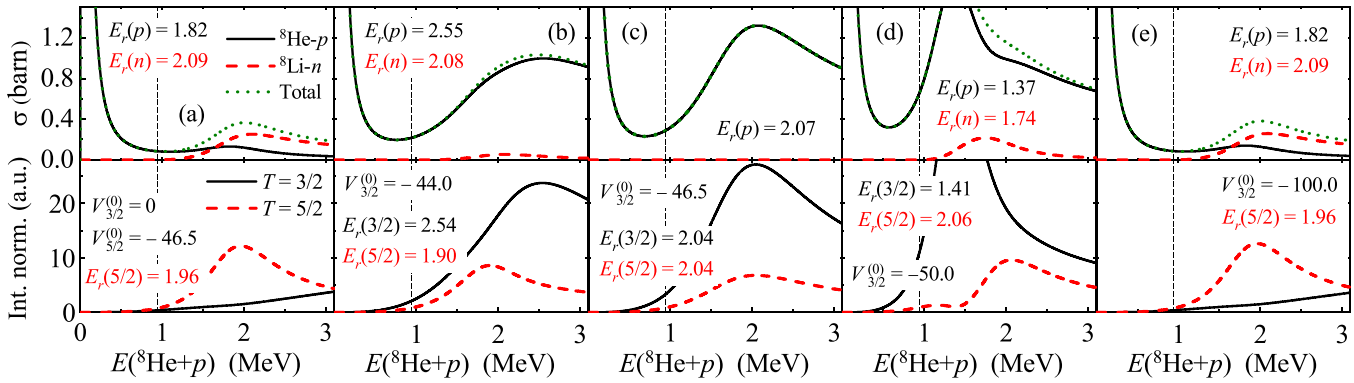

FIG. 2. Upper panels show cross sections for the elastic $^8\text{He}+p$ and inelastic $^8\text{Li}^*(0^+2)+n$ channels. Lower panels show the isospin content of the continuum states in terms of internal normalizations up to 6 fm. Columns (a)–(e) correspond to different cases of $V_{3/2}$ interactions. Value $E_r(i)$ gives the visible peak position in the "i"-th channel. Resonant energy of the $1/2^-$ state in ^{9}He is fixed at $E_r = 1.1$ MeV ($V^{(0)}_{5/2} = -46.5$ MeV, $r_0 = 2.3$ fm). The $^8\text{Li}^*(0^+2)+n$ threshold is shown with vertical dashed lines. All the values of energies in the legends are given in MeV.

By diagonalizing the Schrödinger equation, we get a system of coupled equations

$$\begin{aligned}&[\hat{T} - (E - \Delta E) + (1/5)(V_{3/2} + 4V_{5/2})]\Psi_{^8\text{Li}^*\text{-}n} \\ &\quad + (2/5)(V_{5/2} - V_{3/2})\Psi_{^8\text{He}\text{-}p} = 0, \\ &[\hat{T} - E + V_{\text{coul}} + (1/5)(4V_{3/2} + V_{5/2})]\Psi_{^8\text{He}\text{-}p} \\ &\quad + (2/5)(V_{5/2} - V_{3/2})\Psi_{^8\text{Li}^*\text{-}n} = 0, \end{aligned} \tag{2}$$

where E is the threshold energy in the $^8\text{He}+p$ channel and $\Delta E = 0.941$ MeV is the threshold shift of the $^8\text{Li}^*(0^+2)+n$ channel. We intend to determine the interaction $V_{5/2}$ to fix the spectrum of ^{9}He. However, this can be done only if the $V_{3/2}$ interaction is fixed somehow.

The potentials with the Gaussian form factors $V_T(r) = V^{(0)}_T \exp[-(r/r_0)^2]$ are used in the calculations. The Coulomb interaction of the homogeneously charged sphere is used with radius 2.5 fm, consistent with the charge radius of ^{8}He 1.956(16) fm [23,24]. The potential radius $r_0 \sim 2.0 - 2.4$ fm is fine-tuned establishing condition that the resonant states in both the $^8\text{He}^*(0^+2)+p$ and $^8\text{Li}^*(0^+2)+n$ decoupled channels (case $V_{3/2} \equiv V_{5/2}$) should have the same energy near the $^8\text{He}+p$ threshold. This guarantees that the radial properties of the nucleon orbitals in the $^8\text{He}^*(0^+2)+p$, $^8\text{Li}^*+n$ channels and inside the ^{8}He, $^8\text{Li}^*$ systems are consistent with the threshold energy shift. This is a reasonable isobaric-symmetry requirement.

General features of the model and guidelines for the experiment. The evolution of the $^8\text{He}+p$ scattering with a variation of the $V_{3/2}$ interaction is illustrated in Fig. 2 for the $1/2^-$ continuum. Cross sections for the elastic $^8\text{He}+p$ and inelastic $^8\text{Li}^*(0^+2)+n$ channels are evidently observables, and isospin contents of the continuum states could also be related to observables (e.g., strength functions for isospin-specific reactions).

It can be seen from Eq. (2) that a reduction in the single channel formulation takes place at $V_{3/2} \equiv V_{5/2}$, as seen in Fig. 2(c). It is paradoxical, but such a high "isospin symmetry" leads to isospin degeneracy and mixing. For relatively large differences between the $V_{3/2}$ and $V_{5/2}$ interactions, the isospin symmetry is recovered in our model dynamically and with good precision [see Figs. 2(a) and 2(e)]. In between these limiting situations, the isospin mixing effects are severe and complicated [see Figs. 2(b) and 2(d)], and dynamic calculations are absolutely necessary.

Trajectories in the $\{V_{3/2}, E\}$ plane for the peaks of different observables are summarized in Fig. 3. This is done for three cases of the $1/2^-$ state in the ^{9}He: (a) $E_r = 0.4$, $\Gamma \approx 0.2$ MeV—test case of narrow resonances; (b) $E_r = 1.1$, $\Gamma \approx 0.8$ MeV—as in NNDC (see Fig. 1); and (c) $E_r = 2.1$, $\Gamma \approx 1.9$ MeV—as in Ref. [12]. The following should be noted here:

(i) The scale of energy variation of different peaks with a variation of $V_{3/2}$ interaction is of the order of $\Gamma/2$, which is quite expected. This is a *large* effect for broad states (expected in the ^{9}He case), which cannot be disregarded.

(ii) The deviation in Fig. 3 of peaks that differ from the expected in simple approximation $T = 5/2$ isobaric peak position [dotted lines in Fig. 3: $^8\text{Li}^*(0^+2)+n$ decoupled case] is almost never negligible: the realistic separation of, say, $2-5$ MeV from the $T = 3/2$ state is not sufficient to completely eradicate its effect on the $T = 5/2$ state position observed in different channels.

(iii) The peak values demonstrate "asynchronous" behavior with a variation of $V_{3/2}$. It looks like the $T = 3/2$ state "repels" the $^8\text{He}+p$ continuum and "attracts" the $^8\text{Li}^*(0^+2)+n$ continuum. This "asynchronicity" means that *one single type of data* is not sufficient to understand the actual $T = 5/2$ position, which stays constant in each calculation of Fig. 3. Only the simultaneous studies of the $^8\text{He}+p$ and $^8\text{Li}^*(0^+2)+n$ channels may provide sufficient evidence to fix the $T = 5/2$ properties if we are aiming better than $\Gamma/2$ precision of the method.

The phase shift issue. Important features of the phase shifts obtained in the ICM are illustrated in Fig. 4 for the case of quite narrow $1/2^-$ resonances, which is easiest to perceive. The $T = 5/2$ resonance position is fixed at

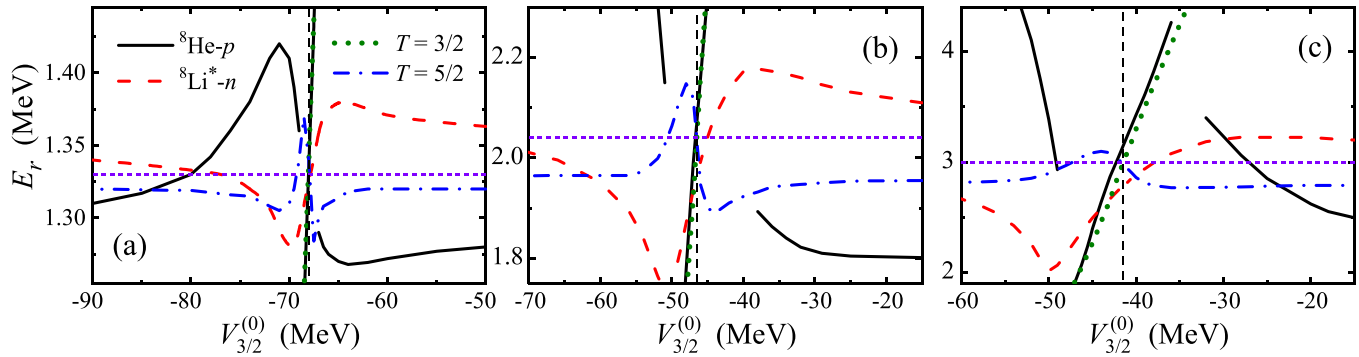

FIG. 3. Trajectories of the peak values for elastic ^{8}He $+p$, inelastic ^{8}Li$^*(0^+2) + n$ channels, and isospin content of the continuum states. Panels (a), (b), and (c) correspond to the resonant energy E_r of the $1/2^-$ state in ^{9}He equal to 0.4, 1.1, and 2.1 MeV, respectively, obtained with $V(0)_{5/2} = \{-68.0, -46.5, -41.5\}$ MeV. The vertical dashed lines indicate the degeneracy situation $V_{3/2} \equiv V_{5/2}$; the horizontal dotted lines show the resonant peak position (from the same threshold) in an elastic ^{8}Li$^*(0^+2) + n$ channel for this case.

$E_r(5/2) = 1.23$ MeV. The use of a somewhat deeper or somewhat weaker $V^{(0)}_{3/2}$ interaction provides the $T = 3/2$ resonance position nearby. One may see that, whatever state is higher in energy—the $T = 3/2$ in Fig. 4(a) or the $T = 5/2$ in Fig. 4(b)—the $T = 3/2$ state demonstrates the "classical" resonant behavior, with the phase shift passing $\pi/2$, while at the $T = 5/2$ resonance energy, only a relatively small "wiggle" in the phase shift is observed. This wiggle is a typical interference pattern for weakly coupled resonance amplitude with exactly $\pi/2$ "initial" relative phase. For the broader states, the $T = 5/2$ wiggles become difficult to identify, while the resonant behavior of the phase at the $T = 3/2$ state energy persists.

The single-channel optical model phase shifts in Ref. [6], and somehow, the combined optical model and R-matrix phase shifts in Ref. [10] were used to analyze the ^{8}He -p data.

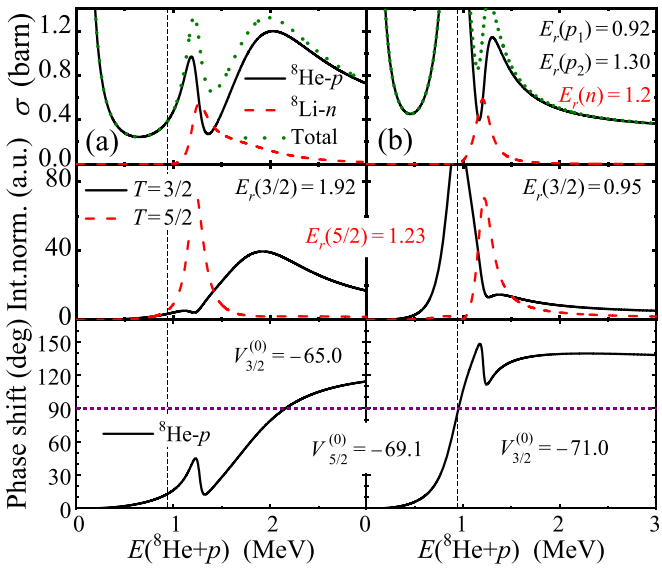

FIG. 4. Cross sections, isospin populations, and phase shifts in the ^{8}He $+p$ channel. Case of $E_r(1/2^-) = 0.3$ MeV in ^{9}He ($V^{(0)}_{5/2} = -69.1$ MeV, $r_0 = 2.0$ fm) and the $V_{3/2}$ interaction providing a small split between $T = 3/2$ and $T = 5/2$ states. Column (a) corresponds to $E_r(5/2) < E_r(3/2)$, and (b) corresponds to $E_r(5/2) > E_r(3/2)$. All the values of energies in the legends are given in MeV.

These approaches rely on a standard resonance identification procedure: the large variation of phase shift passing $\pi/2$ (or close to that). It can be seen in Fig. 4 that, in the model with appropriate isospin treatment, such a behavior is associated only with the $T = 3/2$ states. We have to conclude here that the resonant properties were likely misinterpreted, and the states declared as $T = 5/2$ due to the phase shifts should really be the $T = 3/2$ states. This presumable misinterpretation concerns those listed in NNDC 16.0, 17.1, and 18.9 MeV states of ^{9}Li, all interpreted as $T = 5/2$, and to 2.26, 4.2 MeV states of ^{9}He, inferred by isobaric symmetry (see Fig. 1).

Such phase shift behavior in the ICM is generic. It is always present on some level for proton channels in situation $T > 1$. Therefore, we may foresee the importance of such model studies for analysis of the RPC data on other neutron-rich systems as well.

Discussion of the ^{8}He $+p$ *data interpretation in [10].* In the analysis of that work, the very-close-to-zero phase shifts were deduced for the $p_{1/2}$, $p_{3/2}$, $d_{3/2}$, and $d_{5/2}$ configurations. The $d_{5/2}$ resonance in ^{9}He is expected to be quite high in energy, and its manifestation in the energy window $E(^8\text{He}+p) <$ 3.2 MeV accessible in experiment [10] may be quite small. However, it is surprising that there is no indication of the $p_{1/2}$ resonance at all. It is shown in Fig. 5(a) that, in the ICM, the very small $p_{1/2}$ phases in the whole $E(^8\text{He}+p) < 3$ MeV energy range may be obtained despite the presence in this range of the $p_{1/2}$ resonance with $T = 5/2$, corresponding to the $1/2^-$ resonance in ^{9}He at $E_r \sim 2.1$ MeV. Technically, such a small phase shift in a broad energy range is obtained by combining the "wiggle" feature associated with $T = 5/2$ (rising phase shift trend; see Fig. 4 and related text) with repulsion in the $T = 3/2$ channel (negative and decreasing phase shift in contrast with illustrations in Fig. 4). This situation is consistent with the ^{9}He data of [21], providing $E_r(1/2^-) = 2.0 \pm 0.2$ MeV.

The structured character of the ^{8}He $+p$ cross section in the energy range $0.8 < E(^8\text{He}+p) < 3.2$ MeV is mainly related in the interpretation of Ref. [10] to a curious behavior of the $s_{1/2}$ phase shift. This demonstrates repulsion near the ^{8}He $+p$ threshold, the Wigner cusp at the ^{8}Li$^*(0^+2) + n$ threshold, and $1/2^+$ resonance with $E_r \gtrsim 3.2$ MeV [see Fig. 5(b)]. The latter is interpreted in [10] as corresponding to $1/2^+$

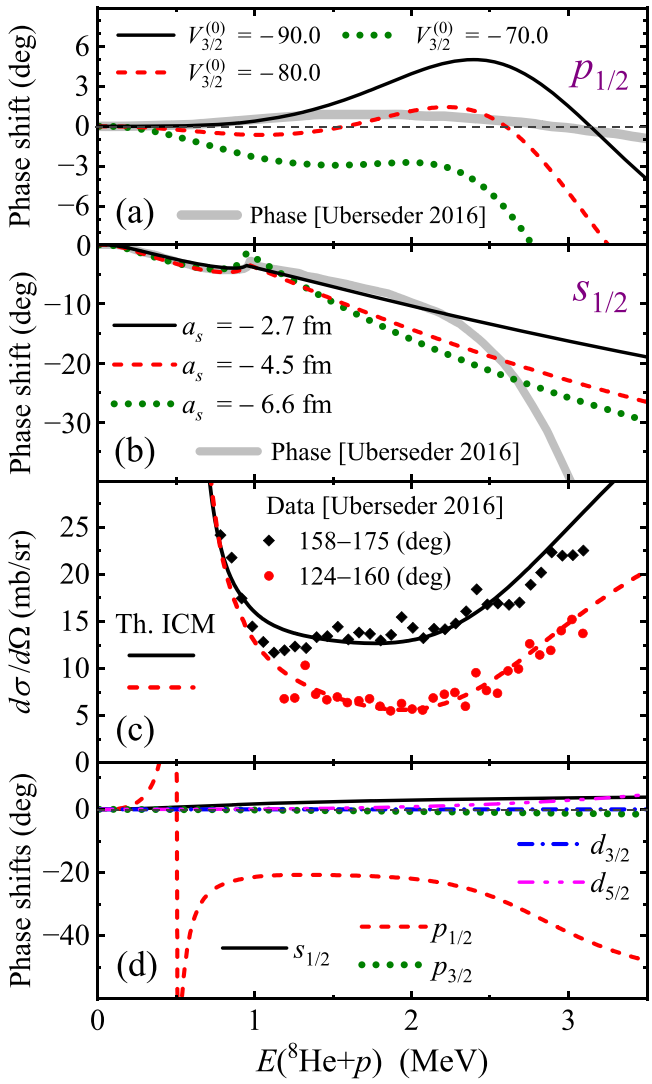

FIG. 5. Panel (a) shows the ICM $p_{1/2}$ phase shifts based on the $T = 5/2$ resonance in ^{9}He $E_r(1/2^-) = 2.1$ MeV ($V_{5/2}^{(0)} = -41.5$ MeV), compared with the phase used to analyze [10]. Panel (b) shows the ICM $s_{1/2}$ phase shifts possessing the Wigner cusp, analogous to that used for the data analysis in Ref. [10]. They are repulsive overall (negative phase shifts), while the $T = 5/2$ interactions are attractive (as indicated in the panel by the negative $T = 5/2$ scattering lengths). The interaction parameters are $V_{3/2}^{(0)} = \{-52, -48, -47\}$ MeV and $V_{5/2}^{(0)} = \{-6.0, -7.5, -8.5\}$ MeV. Panel (c) shows a variant of the ICM analysis of data [10] based on the phases shown in panel (d). The data and fit in (c) for the $124 - 160$ degrees center-of-mass angular range are shown with -5 mb/sr offset to simplify perception. All the values of energies in the legends are given in MeV.

resonance in ^{9}He at $E_r \sim 3$ MeV. It should be noted that the existence of the $s_{1/2}$ resonance in Ref. [10] is directly related to the cusp properties. However, Fig. 5(b) shows that in the ICM, the analogous cusp behavior can be obtained for a variety of situations without any need for $1/2^+$ resonance, including the situation of quite weak attraction in the $1/2^+$ channel, reasonably consistent with the theoretical limitations $a_s \gtrsim 0$ fm deduced in Ref. [22].

Generally, we can obtain in ICM very good fits to the data of Ref. [10]; see, for example, Fig. 5(c). This fit is based on the phases in Fig. 5(d), obtained with the $T = 5/2$ interaction, which is consistent with the ^{9}He data of [21]: weak attraction is $1/2^+$ channel, $1/2^-$ resonance $E_r = 2.3$ MeV, and $5/2^+$ resonance $E_r = 4.7$ MeV. The parameters of the interactions are $V_{3/2}^{(0)} = \{0.0, -55.4, 5.0, 0.0, -60.0\}$ MeV and $V_{5/2}^{(0)} = \{-4.0, -40.5, 5.0, 0.0, -96.5\}$ MeV for the $\{s_{1/2}, p_{1/2}, p_{3/2}, d_{3/2}, d_{5/2}\}$ quantum number sets. We conclude here that the unconventional proposal of [10]—(i) the low-lying $1/2^+$ resonance and (ii) no room for the low-lying $1/2^-$ resonance at all—is actually based on the limited character of the model used in [10], which neglects the complexity of the isospin mixing dynamics.

The data analysis illustrated in Fig. 5(d) is not unique. Other fits of analogous quality are possible, including the cusp-inducing weak repulsion, similar to the cases in Fig. 5(b). Again, we point out that only the additional restrictions from the neutron channel may allow discrimination among different variants.

An important constructive result of our analysis is that, so far, we have found only the $T = 5/2$ interactions providing $E_r(1/2^-) \gtrsim 2.3$ MeV in ^{9}He are tolerated by the data of [10]. This is consistent with the data of [21], providing $E_r(1/2^-) = 2.0 \pm 0.2$ MeV, but not with any other $p_{1/2}$ resonance result (see, e.g., [15] and Refs. therein).

Conclusions. The resonance proton scattering of exotic nuclide on a thick target ^AZ+p in inverse kinematics can be used to infer the properties of the low-energy neutron scattering ^AZ+n on this nuclide by assuming the isobaric symmetry. However, for the relatively broad states and the ^AZ subsystem with nonzero isospin (which is always true for exotic dripline nuclei), the effects of the isospin mixing (due to the $^A(Z+1, \text{IAS}) + n$ channel) and threshold effects are large and should be treated dynamically. This introduces additional uncertainty into the situation: for the ^AZ+n channel, we need only the nuclear cluster interaction with $T_{\max}$, while for the ^AZ+p channel the $T_{\max} - 1$ interaction should also be considered.

The isospin-conserving coupled-channel model is developed to deal with the problem. The effects $T_{\max} - 1$ are shown in this work to be important even for relatively narrow (e.g., $\Gamma \sim 0.3$ MeV) *resonant states*; such treatment is absolutely essential for *broad resonant states* and *s-wave states*. It was demonstrated that the uncertainty connected with $T_{\max} - 1$ interaction can be overcome only if the outgoing $^A(Z+1, \text{IAS}) + n$ channel is studied in parallel with the ^AZ+p elastic channel. There is an example of such neutron channel studies [7], but these are studies of narrow states without simultaneous consideration of the proton channel.

It is predicted within the ICM that the phase shifts of $T_{\max} = 5/2$ and $T_{\max} - 1 = 3/2$ have very distinct behavior. The expected resonant phase shift behavior—with a steep rise and passing $\pi/2$—is found to be common for $T = 3/2$ resonances, not for $T = 5/2$. Thus, resonances of ^{8}He$+p$ identified by this standard approach as $T = 5/2$ in [6] are misidentified. The more recent ^{8}He$+p$ data of [10] can be interpreted within ICM in an alternative and more "orthodox" way: only weak attraction in the $1/2^+$ channel, instead of $s_{1/2}$

resonance, single-particle $1/2^-$ resonance at $E_r = 2.3$ MeV, and $5/2^+$ resonance at $E_r = 4.7$ MeV. This interpretation is consistent with the typical theoretical vision of the ^{9}He spectrum and especially favors the data of [21], which are the only data positioning the $1/2^-$ state sufficiently high in energy. It is thus demonstrated in this work that the results of the resonance proton scattering experiments aimed at the studies of the "isobaric partner" neutron scattering channel may be interpreted in a very different way when isospin conservation is taken properly into account.

Acknowledgments. We are grateful to Prof. E. Yu. Nikolskii and Prof. A. S. Fomichev for important discussions. This work was partly supported by the Russian Science Foundation Grant No. 22-12-00054. The research was partly supported within the framework of a scientific program of the Russian National Center for Physics and Mathematics, Topic No. 6 "Nuclear and radiation physics" (2023–2025 stage). This work was partly supported by MEYS Project LM2023060.

Data Availability. No data were created or analyzed in this study.

[1] V. Z. Gol'dberg, G. Rogachev, M. Golovkov, V. Dukhanov, I. Serikov, and V. Timofeev, JETP Lett. **67**, 1013 (1998).
[2] D. W. Lee, K. Peräjärvi, J. Powell, J. P. O'Neil, D. M. Moltz, V. Z. Goldberg, and J. Cerny, Phys. Rev. C **76**, 024314 (2007).
[3] D. J. Mountford, A. S. Murphy, N. L. Achouri, C. Angulo, J. R. Brown, T. Davinson, F. de Oliveira Santos, N. de Séréville, P. Descouvemont, O. Kamalou, A. M. Laird, S. T. Pittman, P. Ujic, and P. J. Woods, Phys. Rev. C **85**, 022801(R) (2012).
[4] F. de Grancey, A. Mercenne, F. de Oliveira Santos, T. Davinson, O. Sorlin, J. Angelique, M. Assié, E. Berthoumieux, R. Borcea, A. Buta, I. Celikovic, V. Chudoba, J. Daugas, G. Dumitru, M. Fadil, S. Grévy, J. Kiener, A. Lefebvre-Schuhl, N. Michel, J. Mrazek *et al.*, Phys. Lett. B **758**, 26 (2016).
[5] V. Girard-Alcindor, A. Mercenne, I. Stefan, F. de Oliveira Santos, N. Michel, M. Płoszajczak, M. Assié, A. Lemasson, E. Clément, F. Flavigny, A. Matta, D. Ramos, M. Rejmund, J. Dudouet, D. Ackermann, P. Adsley, M. Assunç ao, B. Bastin, D. Beaumel, G. Benzoni *et al.*, Phys. Rev. C **105**, L051301 (2022).
[6] G. V. Rogachev, V. Z. Goldberg, J. J. Kolata, G. Chubarian, D. Aleksandrov, A. Fomichev, M. S. Golovkov, Y. T. Oganessian, A. Rodin, B. Skorodumov, R. S. Slepnev, G. Ter-Akopian, W. H. Trzaska, and R. Wolski, Phys. Rev. C **67**, 041603 (2003).
[7] G. V. Rogachev, P. Boutachkov, A. Aprahamian, F. D. Becchetti, J. P. Bychowski, Y. Chen, G. Chubarian, P. A. DeYoung, V. Z. Goldberg, J. J. Kolata, L. O. Lamm, G. F. Peaslee, M. Quinn, B. B. Skorodumov, and A. Wöhr, Phys. Rev. Lett. **92**, 232502 (2004).
[8] F. De Oliveira Santos, I. Stefan, and J.-C. Dalouzy, Int. J. Mod. Phys. E **18**, 2140 (2009).
[9] C. Hunt, G. V. Rogachev, S. Almaraz-Calderon, A. Aprahamian, M. Avila, L. T. Baby, B. Bucher, V. Z. Goldberg, E. D. Johnson, K. W. Kemper, A. N. Kuchera, W. P. Tan, and I. Wiedenhöver, Phys. Rev. C **102**, 014615 (2020).
[10] E. Uberseder, G. Rogachev, V. Goldberg, E. Koshchiy, B. Roeder, M. Alcorta, G. Chubarian, B. Davids, C. Fu, J. Hooker, H. Jayatissa, D. Melconian, and R. Tribble, Phys. Lett. B **754**, 323 (2016).
[11] C. Hunt, S. Ahn, J. Bishop, E. Koshchiy, E. Aboud, M. Alcorta, A. Bosh, K. Hahn, S. Han, C. E. Parker, E. C. Pollacco, B. T. Roeder, M. Roosa, S. Upadhyayula, A. S. Volya, and G. V. Rogachev, Phys. Rev. C **108**, L051606 (2023).
[12] M. S. Golovkov, L. V. Grigorenko, A. S. Fomichev, A. V. Gorshkov, V. A. Gorshkov, S. A. Krupko, Y. T. Oganessian, A. M. Rodin, S. I. Sidorchuk, R. S. Slepnev, S. V. Stepantsov, G. M. Ter-Akopian, R. Wolski, A. A. Korsheninnikov, E. Y. Nikolskii, V. A. Kuzmin, B. G. Novatskii, D. N. Stepanov, P. Roussel-Chomaz, and W. Mittig, Phys. Rev. C **76**, 021605(R) (2007).
[13] L. V. Grigorenko, N. B. Shul'gina, and M. V. Zhukov, Nucl. Phys. A **665**, 105 (2000).
[14] L. V. Grigorenko, B. V. Danilin, and N. B. Shul'gina, Nucl. Phys. A **671**, 136 (2000).
[15] T. Al Kalanee, J. Gibelin, P. Roussel-Chomaz, N. Keeley, D. Beaumel, Y. Blumenfeld, B. Fernández-Domínguez, C. Force, L. Gaudefroy, A. Gillibert, J. Guillot, H. Iwasaki, S. Krupko, V. Lapoux, W. Mittig, X. Mougeot, L. Nalpas, E. Pollacco, K. Rusek, T. Roger *et al.*, Phys. Rev. C **88**, 034301 (2013).
[16] D. Votaw, P. A. DeYoung, T. Baumann, A. Blake, J. Boone, J. Brown, D. Chrisman, J. E. Finck, N. Frank, J. Gombas, P. Guèye, J. Hinnefeld, H. Karrick, A. N. Kuchera, H. Liu, B. Luther, F. Ndayisabye, M. Neal, J. Owens-Fryar, J. Pereira *et al.*, Phys. Rev. C **102**, 014325 (2020).
[17] D. Tilley, J. Kelley, J. Godwin, D. Millener, J. Purcell, C. Sheu, and H. Weller, Nucl. Phys. A **745**, 155 (2004).
[18] L. Chen, B. Blank, B. Brown, M. Chartier, A. Galonsky, P. Hansen, and M. Thoennessen, Phys. Lett. B **505**, 21 (2001).
[19] H. T. Johansson, Y. Aksyutina, T. Aumann, K. Boretzky, M. Borge, A. Chatillon, L. V. Chulkov, D. Cortina-Gil, U. D. Pramanik, H. Emling, C. Forssen, H. O. U. Fynbo, H. Geissel, G. Ickert, B. Jonson, R. Kulessa, C. Langer, M. Lantz, T. LeBleis, K. Mahata *et al.*, Nucl. Phys. A **842**, 15 (2010).
[20] H. Al Falou, A. Leprince, and N. Orr, J. Phys.: Conf. Ser. **312**, 092012 (2011).
[21] M. S. Golovkov, L. V. Grigorenko, G. M. Ter-Akopian, A. S. Fomichev, Y. T. Oganessian, V. A. Gorshkov, S. A. Krupko, A. M. Rodin, S. I. Sidorchuk, R. S. Slepnev, S. V. Stepantsov, R. Wolski, D. Y. Pang, V. Chudoba, A. A. Korsheninnikov, E. A. Kuzmin, E. Y. Nikolskii, B. G. Novatskii, D. N. Stepanov, P. Roussel-Chomaz *et al.*, Phys. Lett. B **672**, 22 (2009).
[22] P. G. Sharov, I. A. Egorova, and L. V. Grigorenko, Phys. Rev. C **90**, 024610 (2014).
[23] P. Mueller, I. A. Sulai, A. C. C. Villari, J. A. Alcántara-Núñez, R. Alves-Condé, K. Bailey, G. W. F. Drake, M. Dubois, C. Eléon, G. Gaubert, R. J. Holt, R. V. F. Janssens, N. Lecesne, Z.-T. Lu, T. P. O'Connor, M.-G. Saint-Laurent, J.-C. Thomas, and L.-B. Wang, Phys. Rev. Lett. **99**, 252501 (2007).
[24] J. J. Krauth, K. Schuhmann, M. A. Ahmed, F. D. Amaro, P. Amaro, F. Biraben, T.-L. Chen, D. S. Covita, A. J. Dax, M. Diepold, L. M. P. Fernandes, B. Franke, S. Galtier, A. L. Gouvea, J. Gotzfried, T. Graf, T. W. Hansch, J. Hartmann, M. Hildebrandt, P. Indelicato *et al.*, Nature (London) **589**, 527 (2021).